Journal of System Design and Dynamics

Vol. 2, No. 4, 2008

Application of Momentum Exchange Impact Dampers to Forging Machine*

Lovely SON**, Daisaku NAKATANI**, Hiroshi MATSUHISA** and Hideo UTSUNO**

**Department of Precision Engineering, Kyoto University, Yoshidahonmachi, Sakyo-ku, Kyoto 606-8501, Japan

E-mail: lovelyson@std.mbox.media.kyoto-u.ac.jp

Abstract

This paper proposes an impact control method for a forging machine using a momentum exchange impact damper. This method is based on momentum conservation of two colliding bodies. A conventional added mass control method fails to suppress the acceleration and force transmission simultaneously. By using the momentum exchange impact damper, it is shown that the bed acceleration and the transmitted force to the floor are reduced. This paper presents a theoretical analysis of an impact damper and an optimum condition that leads to a minimization of the energy of a forging machine. An experimental analysis is shown to validate the simulation results.

Key words: Damper, Impact, Vibration Control, Momentum Exchange, Forging Machine

1. Introduction

Industrial machines using impact force, such as forging machine, have two dominant problems relating to their dynamic operation. The first problem relates to the inertial force caused by rigid-body motion of the machines, which is excited by its reciprocating movement. The second problem relates to elastic vibration caused by the impacts. These problems reduce the machines accuracy and cause vibration pollution to the surroundings.

Conventional methods of addressing these problems typically involve using a floating base with a large mass to decrease the transmitted force. These methods fail to improve the vibration response of the forging machine bed. Tanaka [1,2] proposed a novel technique to address these problems by using an active damper with preview action, which reduced the transient vibration due to the impact. This method effectively reduces the transmitted force and the acceleration response. However, it requires sensors, a controller, and an actuator to realize the preview action of the dynamic damper.

In this paper, an innovative momentum exchange impact damper is proposed to reduce the vibration and transmitted force of the forging machine. This method is based on the momentum conservation principle for colliding bodies [3,4]. When the forging machine bed is subjected to an impact force, a part of the energy of the forging machine is transferred to the impact damper mass, which is initially in contact with the forging machine bed.

The energy transfer analysis is conducted to evaluate the effectiveness of the damper in reducing the shock energy. In this analysis, the energy of a forging machine after the shock is calculated and evaluated with variation of forging machine parameters such as the contact condition and the mass ratio. The simulation results show that the energy being transferred to the damper is largely dependent on the contact condition and the mass ratio. In addition, three configurations of forging machine with the impact damper are evaluated in this paper.

*Received 5 June, 2007 (No. 07-0241)
[DOI: 10.1299/jsdd.2.1027]

In the first configuration, the forging machine uses the floating base with low support stiffness. For this configuration, the floating mass is much larger than the mass of forging machine bed. In the second configuration, the forging machine uses the floating base with high support stiffness. In the last configuration, the forging machine is evaluated without using a floating base.

2. New Impact Damper for Forging Machine

Figure 1 shows a dynamic model of a forging machine with an impact damper. There are four main components in this system. The first component is a slider, which is used as the impact force generator for the forging machine. The second component is the bed. The bed typically consists of a steel plate supported by four columns. These columns connect the forging machine bed to the third component, a floating base. The floating base is a steel plate supported by four coil springs. The last component is the impact damper. The impact damper consists of a mass which is supported by a spring and a dashpot.

The slider, the bed and the damper mass contact directly, however the contact conditions are simulated by linear springs and linear dampers as shown in Fig. 1.

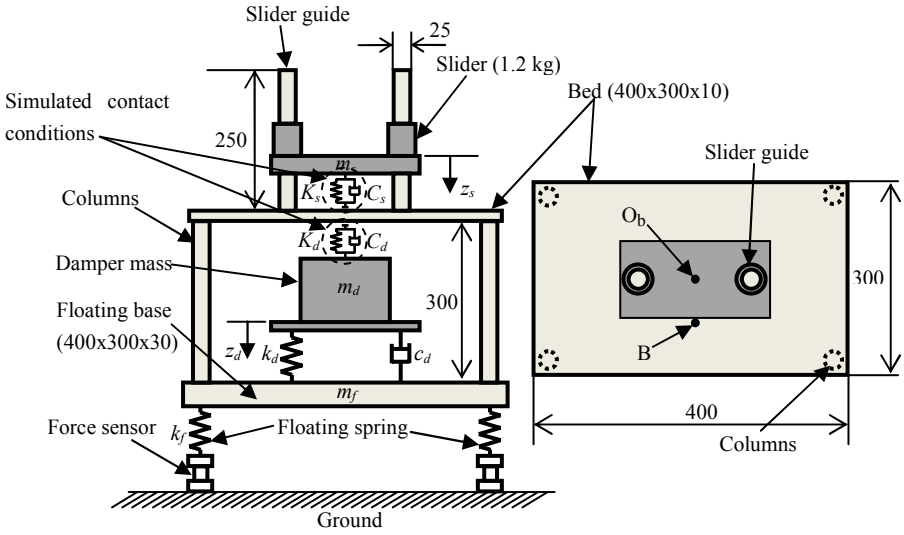

Fig. 1 Dynamic model of a forging machine.

3. System Modeling and Equations of Motion

The dynamics of the forging machine structure, which consists of the slider guides, a bed, columns, a floating base, and floating base springs, is analyzed using the finite element method (FEM). Four-node quadrilateral plate elements are used to model both the bed and the floating base structure [5]. The columns are modeled using three dimensional frame elements [6]. The slider and the impact damper are assumed to be rigid bodies.

Values for defining the slider, the bed, the impact damper and the floating base parameters are shown in Table 1. The equations of motion of the forging machine structure, the slider, and the impact damper are written as follows

$$\mathbf{M}\ddot{\mathbf{u}} + \mathbf{C}\dot{\mathbf{u}} + \mathbf{K}\mathbf{u} = \mathbf{B}_{\mathbf{bs}} f_{bs} - \mathbf{B}_{\mathbf{bd}} f_{bd} + \mathbf{B}_{\mathbf{fd}} f_{fd}, \quad (1)$$

$$m_s \ddot{z}_s + f_{bs} = 0, \quad (2)$$

$$m_d \ddot{z}_d + f_{fd} - f_{bd} = 0, \quad (3)$$

Table 1 Simulation parameters for slider, bed, damper and floating base

Parameter	Value
m_s : slider mass	1.2 kg
v_s : slider initial velocity	1.2 m/s
m_b: bed mass	10 kg
K_s : bed-slider contact stiffness	1.0×10^6 – 5.0×10^7 N/m
C_s : bed-slider contact damping coefficient	0 Ns/m
m_d : damper mass	3.6 kg, 7.2 kg
k_d : damper spring constant	1.8×10^3 N/m
c_d : damper damping coefficient	7.0×10^2 Ns/m
K_d: bed-damper contact stiffness	5.5×10^3 – 1.8×10^9 N/m
C_d : bed-damper contact damping coefficient	0 Ns/m
m_f : floating base mass	41 kg
k_f: floating base spring constant	1.5×10^4 N/m, 1.0×10^7 N/m

where matrix **M**, **C** and **K** are the structure's mass matrix, the damping matrix, and the stiffness matrix, respectively; f_{bs}, f_{bd} and f_{fd} are the contact force between the bed and the slider, the contact force between the bed and the impact damper and the transmitted force from the impact damper to the floating base, respectively; **u**, z_s and z_d are the displacement vectors of the structure, the displacement of slider, and the displacement of the impact damper, respectively; and $\mathbf{B_{bs}}$, $\mathbf{B_{bd}}$ and $\mathbf{B_{fd}}$ are vectors that represent the positions of external forces. The **u** vector consists of three components:

$$\mathbf{u}=\left[\mathbf{u}_{\mathbf{bg}}^{\mathrm{T}},\mathbf{u}_{\mathbf{cg}}^{\mathrm{T}},\mathbf{u}_{\mathbf{fg}}^{\mathrm{T}}\right]^{\mathrm{T}}, \tag{4}$$

where $\mathbf{u_{bg}}$, $\mathbf{u_{cg}}$ and $\mathbf{u_{fg}}$ are the global coordinate displacement vectors of the bed, column and floating base, respectively. The superscript T in Eq. (4) denotes the transpose operation.

The contact force between the bed and slider is assumed to be given by a linear spring and a dashpot [7]. Thus, the contact force can be expressed as

$$f_{bs}=\begin{cases}K_s\left(z_s-u_b\right)+C_s\left(\dot{z}_s-\dot{u}_b\right), & for\ \left(z_s-u_b\right)\geq 0\\ 0, & for\ \left(z_s-u_b\right)<0\end{cases}, \tag{5}$$

where K_s and C_s are the contact stiffness and the contact damping coefficient between the slider and the bed, respectively, while u_b is the displacement of the bed at the contact point O_b. The transmitted force from the impact damper to the floating base can be expressed as

$$f_{fd}=c_d(\dot{z}_d-\dot{u}_f)+k_d(z_d-u_f), \tag{6}$$

where k_d and c_d are the stiffness and the damping coefficients of the impact damper, respectively, while u_f is the displacement of the floating base at the center point O_f. The impact damper is designed such that it moves smoothly during the impact such that it dissipates energy when it releases. A one-way damper is used for this purpose. Mathematically, the damping coefficient can be expressed as

$$c_d=0 \quad for\ \ \dot{z}_d-\dot{u}_f>0\ . \tag{7}$$

The contact force between the bed and the impact damper is modeled using a linear spring and dashpot model

$$f_{bd}=\begin{cases}K_d\left(u_b-z_d\right)+C_d\left(\dot{u}_b-\dot{z}_d\right), & for\ \left(u_b-z_d\right)\geq 0\\ 0, & for\ \left(u_b-z_d\right)<0\end{cases}, \tag{8}$$

where C_d and K_d are the contact damping coefficient and the contact stiffness between the

impact damper and the bed, respectively.

Equation (1) can be written in modal coordinates giving

$$\ddot{q}_i + 2\zeta_i\omega_i\dot{q}_i + \omega_i^2 q_i = \boldsymbol{\psi}_i\left[\mathbf{B}_{\mathbf{bs}}f_{bs} - \mathbf{B}_{\mathbf{bd}}f_{bd} + \mathbf{B}_{\mathbf{fd}}f_{fd}\right] \quad , \quad \mathrm{i} = 1,2,\cdots,\infty \, , \qquad (9)$$

where q_i, ζ_i, ω_i, and $\boldsymbol{\psi}_\mathrm{i}$ are the modal displacements, the damping ratio, the natural frequency and the mass normalized eigenvector for the ith mode, respectively.

Figure 2 shows two mode shapes of the forging machine without a damper obtained from the FEM. The 6th and the 10th modes significantly contribute to the transfer of energy during the collision process. The 6th mode is the rigid body mode of forging machine and the 10th mode is the most dominant elastic mode of bed.

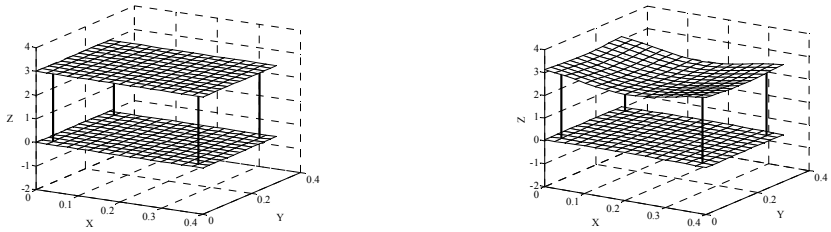

(a) 6th mode (6.35 Hz) (b) 10th mode (283 Hz)

Fig. 2 Significant mode shapes of the bed, column and floating base.

4. Energy Transfer and Transmitted Force

The main purpose of the impact damper is to minimize the momentum or energy of the forging machine. Generally, the transfer of momentum in the collision of elastic bodies is influenced by the mass ratio and the contact time. In order to find the optimum mass ratio and contact stiffness, several simulations were conducted. In the simulations, the energy of the forging machine after collisions are calculated as

$$E_{p+} = E_{s-} - E_{s+} - E_{d+} \quad , \qquad (10)$$

where E_{p+}, E_{s-}, E_{s+} and E_{d+} are the energy of the forging machine after collision, the energies of the slider before and after collision, and the energy of the impact damper after collision, respectively. These energies are calculated as

$$E_{s-} = T_{s-} = \frac{1}{2}m_s\dot{z}_{s-}^2 \quad , \qquad (11)$$

$$E_{s+} = T_{s+} = \frac{1}{2}m_s\dot{z}_{s+}^2 \quad , \qquad (12)$$

$$E_{d+} = T_{d+} + U_{d+} = \frac{1}{2}m_d\dot{z}_{d+}^2 + \frac{1}{2}k_d\left(z_d - u_f\right)_+^2 \quad , \qquad (13)$$

where $\dot{z}_{s-}$, $\dot{z}_{s+}$, $\dot{z}_{d+}$ and $(z_d - u_f)_+$ are velocities of the slider before and after collision, velocity of the damper after collision, and relative displacement of the damper after collision, respectively. T_{s-}, T_{s+}, T_{d+}, and U_{d+} are the kinetic energies of the slider mass before and after collision, kinetic energy of the damper mass after collision, and potential energy of the damper spring after collision, respectively. It can be assumed that there is no potential energy just after the collision.

The analysis of energy transfer from the slider to the damper was conducted for three different cases. For the first case, the forging machine was supported by a floating base with a soft support spring ($k_f = 1.5 \times 10^4$ N/m). The natural frequency of rigid body vibration mode in this case is much smaller than the natural frequency of the bed. In the second case, the

forging machine is supported by a floating base with a hard support spring (k_f = 1.0× 10^7 N/m). The natural frequency of the rigid body vibration in this case is higher than that of the first case. In the last case, the forging machine column was connected rigidly to the ground without using a floating base.

4.1 Case 1: Using Floating Base with Low Support Stiffness

The numerical integration of Eqs. (2), (3) and (9) was carried out in a MATLAB/Simulink computational environment by using the fifth-order Dormand-Prince method with variable time steps. In the simulation, only the 6th mode (ω_6 = 40 rad/s) and 10th mode (ω_{10} = 1777 rad/s) were considered, because they were dominant. Figure 3 shows the ratio of transferred energy (E_{p+}/E_{s-}) as a function of ω_s/ω_6 and ω_d/ω_6 for mass ratios (m_d/m_b) of 0.35 and 0.7. The variables, ω_s and ω_d, are the contact frequencies of the slider and the impact damper,

$$\omega_s = \sqrt{\frac{K_s}{m_s}} \quad , \tag{14}$$

$$\omega_d = \sqrt{\frac{K_d}{m_d}} \quad . \tag{15}$$

These variables relate to the contact time with the bed.

As can be seen from Fig. 3, the minimum energy of the forging machine occurs in the neighborhood of the point where $\omega_d = \omega_s$. This energy decreases when the frequency ratio ω_s/ω_6 is increased. The conclusion that can be drawn from these figures is that K_s must be higher in order to minimize the energy of the forging machine.

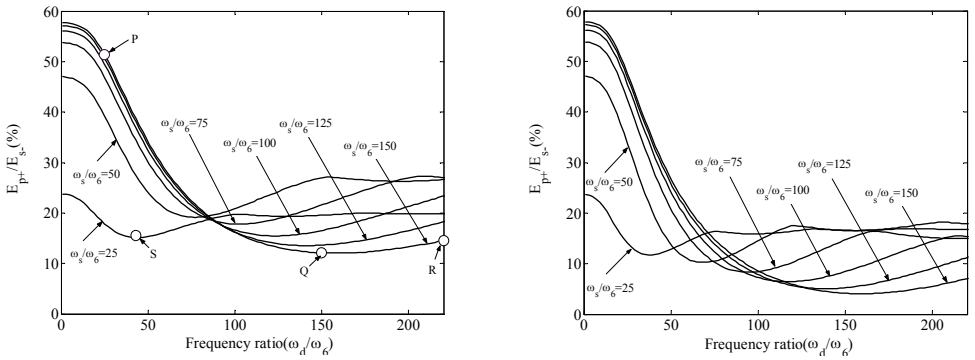

(a) m_d/m_b = 0.35 (b) m_d/m_b = 0.7

Fig. 3 Relationship between energy transfer and contact condition.

Figure 4 shows the variation of the forging machine energy ratio with the frequency ratio ω_d/ω_s and the impact damper mass ratio m_d/m_b. In the simulation, ω_s and ω_6 were fixed to be 6× 10^3 rad/s and 40 rad/s, respectively, and the contact frequency ω_d was varied. It shows that the large m_d is effective to reduce the energy of forging machine. The minimum energy is located at ω_d/ω_s = 1 for all mass ratios. Considering the energy ratio E_{p+}/E_{s-} as impact damper efficiency, it can be concluded that the optimal frequency ratio ω_d/ω_s that is close to 1 is independent of the impact damper mass. For the optimal impact damper with a mass ratio of 1, E_{p+}/E_{s-}= 2.2 % as shown in Fig. 4.

Figure 5 shows the variation of the forging machine energy ratio with the frequency ratio ω_s/ω_6 and the mass ratio m_d/m_b. In this simulation the natural frequency was fixed to

be $\omega_6 = 40$ rad/s and the contact frequency ω_s and ω_d were varied. During the simulation, the contact frequency ω_d was set to the same value as ω_s and m_s was kept constant. The curves for the energy have a maximum peak at the point close to $\omega_s/\omega_6 = 45$ (ω_s : 283 Hz). This was because the natural frequency of the 10th mode of the forging machine (ω_{10}) is 283 Hz and this value is the same as the contact frequency ω_s. At this point, the energy of the forging machine increases due to resonance. When the forging machine operates at $\omega_s/\omega_6 < 45$, the impact damper mass ratio has little influence on the energy of the forging machine as shown in Fig. 5. However, for $\omega_s/\omega_6 > 45$, the mass ratio has a significant effect in determining the energy of forging machine after the impact. This is because, for $\omega_s/\omega_6 < 45$, the slider contact stiffness is so small that the amount of energy reflected to the slider is larger than the amount transferred. In this condition the mass ratio has little influence on the amount of reflected energy. When $\omega_s/\omega_6 >> 45$, the energy transferred to the damper increases and this transferred energy is influenced greatly by the mass ratio.

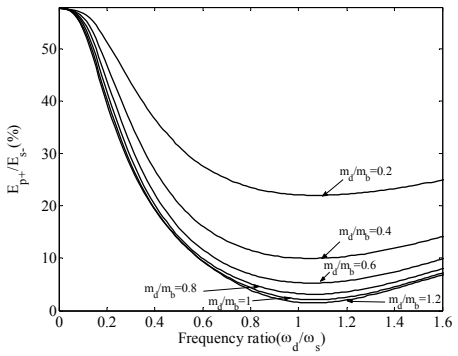

Fig. 4 Relationship between energy transfers and mass ratio.

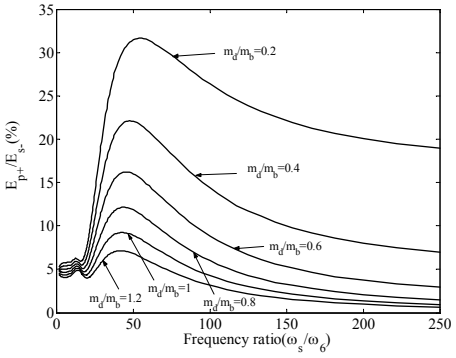

Fig. 5 Variation of energy ratio with frequency ratio ω_s/ω_6 and mass ratio m_d/m_b.

The time history of the energy during collision for a mass ratio of 0.35 and $\omega_s/\omega_6 = 150$ are depicted in Figs. 6-8. The energy components in Figs. 6-8 are calculated as follows.

1. The kinetic energy of the slider is

$$KE\,m_s = \frac{1}{2} m_s \dot{z}_s^2 \quad . \tag{16}$$

2. The potential energy stored internally in the slider contact spring is

$$PE\,K_s = \frac{1}{2} K_s \left| \left(z_s - u_b \right)^2 \right| \times \frac{1}{2} \left(1 - \mathrm{sgn}\left(z_s - u_b \right) \right) . \tag{17}$$

3. The kinetic energy and potential energy of the forging machine

$$KE_p = \frac{1}{2} \{\dot{\mathbf{X}}\}^{\mathrm{T}} [\mathbf{M}] \{\dot{\mathbf{X}}\} , \tag{18}$$

$$PE_p = \frac{1}{2} \{\mathbf{X}\}^{\mathrm{T}} [\mathbf{K}] \{\mathbf{X}\} , \tag{19}$$

where $\{\mathbf{M}\}$, $\{\mathbf{K}\}$, $\{\mathbf{X}\}$ and $\{\dot{\mathbf{X}}\}$ are the modal mass, the modal stiffness, the displacement vector and the velocity vector of the forging machine, respectively.

4. The kinetic energy of the damper is

$$KE\,m_d = \frac{1}{2} m_d \dot{z}_d^2 \quad . \tag{20}$$

5. The potential energy stored in the damper spring is

$$PE\;k_d = \frac{1}{2} k_d \left(z_d - u_f \right)^2 . \tag{21}$$

6. The potential energy stored internally by the damper contact spring is

$$PE\,K_d = \frac{1}{2}K_d\left|\left(u_b - z_d\right)^2\right| \times \frac{1}{2}\left(1 - \mathrm{sgn}\left(u_b - z_d\right)\right). \quad (22)$$

7. Energy dissipated by the forging machine structural damping is given by

$$Dissipated\ energy = KE\,m_{s-} - \left[PE\,K_s + KE\ structure + PE\ structure + KE\,m_d + PE\,k_d + PE\,K_d\right], \quad (23)$$

where $KE\ m_{s-}$ is the kinetic energy of the slider before collision.

It should be noted that the energy of the forging machine is the summation of kinetic energy, potential energy, and dissipated energy.

$$E_p = KE_P + PE_p + Dissipated\ energy. \quad (24)$$

Calculation of the energy components is conducted for ω_s/ω_6=150. Figures 6, 7, and 8 show the time history of energy for ω_d/ω_6=150 (point Q in Fig. 3 (a)), ω_d/ω_6=25 (point P in Fig. 3(a)) and ω_d/ω_6=220 (point R in Fig. 3(a)). Compared to the kinetic energy at point P and point R, the kinetic energy of the damper at point Q is much larger. This occurs because when the contact takes place, there is a steady drop in the kinetic energy of the slider ($KE\ m_s$) as a result of energy transfer to the other energy compartments ($PE\ K_s$, $PE\ K_d$, $KE\ m_d$ and E_p). The portion of energy transferred into the kinetic energy of the impact damper ($KE\ m_d$) is greatly influenced by the amount of potential energy stored in the impact damper contact spring ($PE\ K_d$). Figure 6 shows that when the impact damper works at point Q, the maximum value of $PE\ K_d$ occurs at the same time at which the slider losses contact.

When the impact damper is working at point P, as shown in Fig. 7, the kinetic energy of the impact damper after collision is smaller than that at point Q. This occurs because in this case the maximum value of $PE\ K_d$ occurs after the slider losses contact. Alternatively, when the damper works at point R, the maximum value of $PE\ K_d$ occurs before the slider looses contact, so that the kinetic energy of the impact damper is lower than that at point Q.

The conclusion that can be reached from the above analysis is that the maximum energy transfer from the slider to the impact damper is obtained if the time when $PE\ K_d$ is at a maximum and the time when slider looses contact are the same.

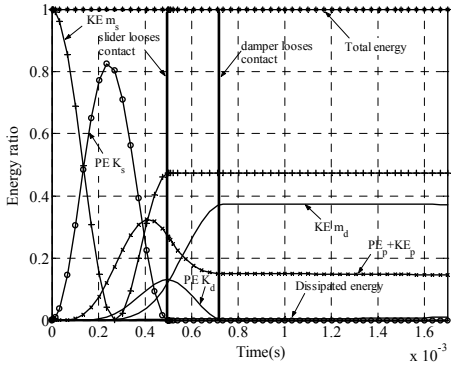

Fig. 6 Energy time history for m_d/m_b =0.35, ω_s/ω_6=150 and ω_d/ω_6=150 (point Q).

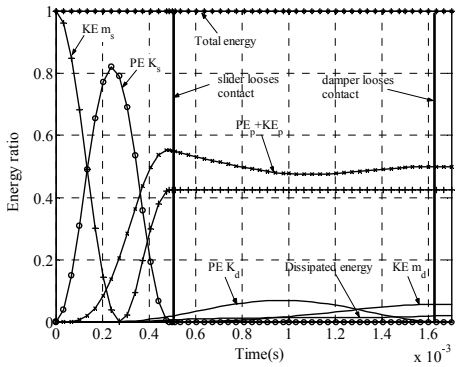

Fig. 7 Energy time history for m_d/m_b =0.35, ω_s/ω_6=150 and ω_d/ω_6=25 (point P).

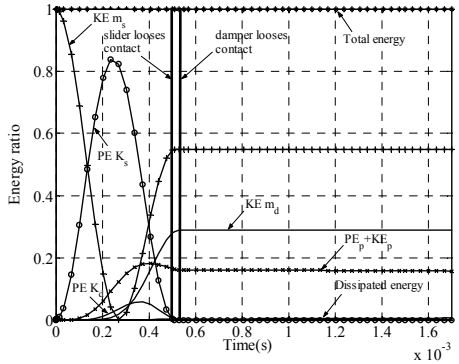

Fig. 8 Energy time history for m_d/m_b =0.35, ω_s/ω_6=150 and ω_d/ω_6=220 (point R).

One of the conventional ways to reduce impact vibration is to add a mass on the bed or floating base. Comparison of the performance of the impact damper with the conventional added mass method is depicted in Fig. 9. In this simulation the weight of the added mass is the same as that of the impact damper with a mass ratio 0.35. The frequency ratio of the impact damper is ω_d/ω_s=1. Figure 9 shows that the impact damper has a better performance compared to the added mass method in the whole frequency range defined by the impact stiffness (ω_s/ω_6).

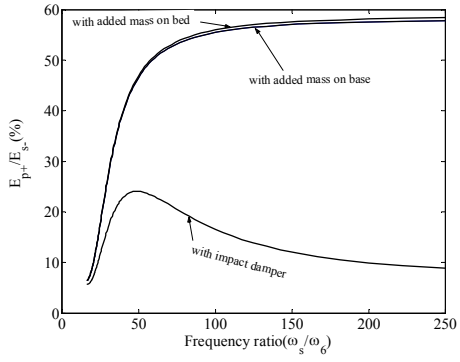

Fig. 9 Comparison between added mass and impact damper method.

Figure 10 and 11 show the simulated acceleration of the bed and transmitted force to the ground at the operating point S (see Fig. 3 (a)) for three cases: without impact damper, with impact damper, and with added mass on the base. The added mass and the impact damper mass are $m_d/m_b = m_{add}/m_b$ = 0.35. The acceleration and the transmitted force for the impact damper case are less than without the impact damper and the added mass cases. The

added mass case has low transmitted force, but the acceleration response is poor compared to the impact damper case. Note that the acceleration response is dominated by the elastic mode of the bed (283 Hz). Meanwhile the transmitted force is dominated by the rigid body vibration (6.35 Hz).

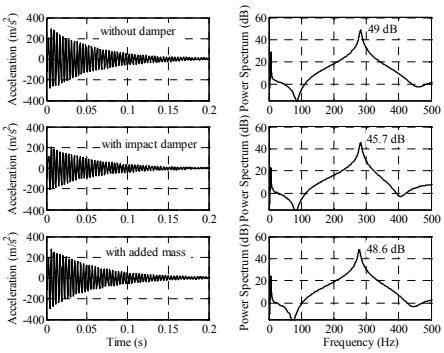

Fig. 10 Simulated acceleration response at point S.

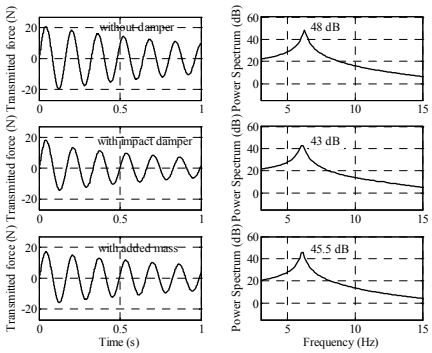

Fig. 11 Simulated force transmission at point S.

4.2 Case 2: Using Floating Base with High Support Stiffness

Figure 12 shows the forging machine energy obtained from the simulation by using a floating base stiffness $k_f = 1.0 \times 10^7$ N/m. This stiffness value is much larger than the stiffness used in the previous simulation. By using this spring, the 6th and 10th natural frequencies of the forging machine become 141 Hz and 292 Hz, respectively, while in the case of $k_f = 1.5 \times 10^4$ they are 6.35 Hz and 283 Hz. The mass ratio in this simulation is 0.35. Compared to the case with $k_f = 1.5 \times 10^4$ in Fig. 3 (a), the shapes of energy curve are similar and the minimum point is located in the vicinity of $\omega_d = \omega_s$.

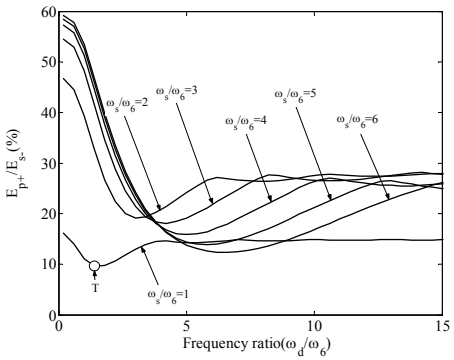

Fig. 12 Relationship between energy transfer and contact condition for $K_f = 1.0 \times 10^7$.

Figure 13 and Fig. 14 show the response of the bed acceleration and transmitted force at the operating point T in Fig. 12. The contact stiffness between slider and bed (K_s) at point T is the same as K_s at point S in Fig. 3 (a). It can be shown from these figures that the acceleration and transmitted force are less than those in the case with the soft support spring because most of energy of the slider is reflected back to the slider after the impact. By using the impact damper, the acceleration and transmitted force can be reduced by about 3 dB.

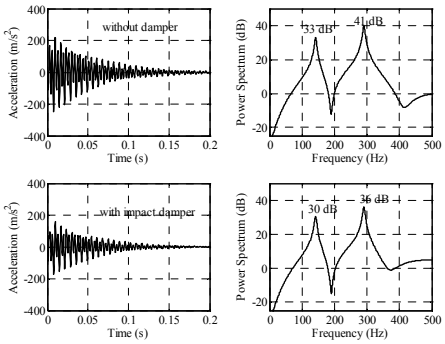

Fig. 13 Simulated acceleration at point T.

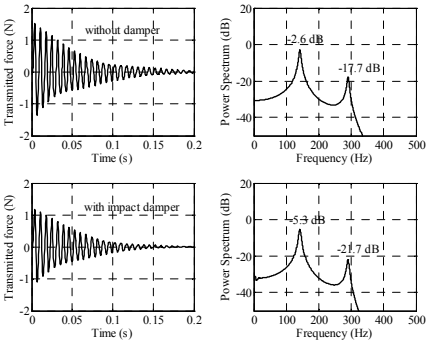

Fig. 14 Simulated force transmission at point T.

4.3 Case 3: Without Using a Floating Base

In the case of small forging machines, the columns are usually connected directly to the ground without using a floating base. The transmitted force is simply calculated from the column's deflection ($F_t = k_c x_c$ where k_c and x_c are the stiffness and deflection of column, respectively). Several mode shapes of forging machines without floating base are depicted in Fig. 15. It can be shown from these figures that the 4th and 5th modes are significant for the case when the excitation point is located at the center of the bed.

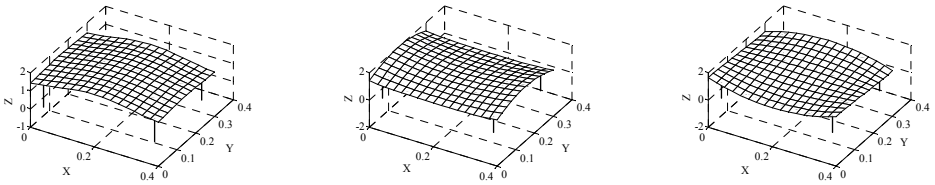

(a) 4th mode, 216 Hz (b) 5th mode, 275.6Hz (c) 6th mode, 281 Hz

Fig. 15 The significant mode shapes of forging machine without floating base.

Figure 16 shows the variation of forging machine energy of using the impact damper for cases without a floating base. The energy of forging machine is minimum at a point close to $\omega_s = \omega_d$ as shown in Fig. 16.

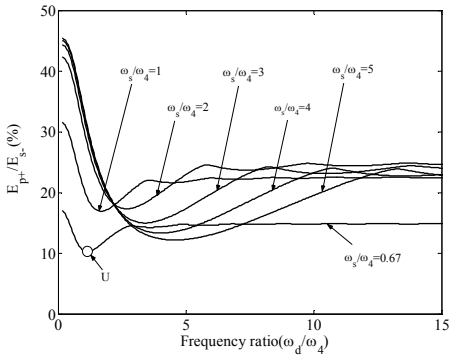

Fig. 16 Relationship between energy transfer and contact condition without a floating base.

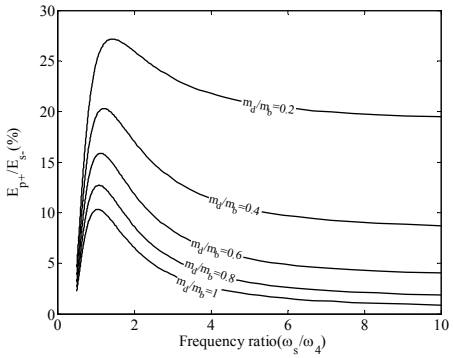

Fig. 17 Variation of energy with frequency ratio ω_s/ω_4 and mass ratio m_d/m_b.

Figure 17 shows the variation of energy with frequency ratio ω_s/ω_4 and mass ratio

m_d/m_b. In this simulation the contact frequency ω_s and ω_d were varied. During the simulation, the contact frequency ω_d was set to the same value as ω_s and m_s was held constant. The energy curve has a maximum peak at the point close to $\omega_s/\omega_4 = 1$ because the resonance occurs when the excitation frequency ω_s is the same as the bed natural frequency ω_4.

The forging machine energy for the third case depends strongly on the transfer of momentum from the slider to the impact damper. Compared to the case with a floating base, the forging machine energy for this case is much lower.

The acceleration response at the center of bed and the transmitted force from the column to the ground at the operating point U (see Fig. 16) are depicted in Fig. 18 and Fig. 19. Figure 18 shows that the 4th mode of the forging machine has the most dominant peak. The peak for the 5th mode is small compared to the peak of the 4th mode. The attenuation of the peak acceleration by the impact damper with a mass ratio of 0.35 is 2.3dB. The response of transmitted force from the column to the ground is depicted in Fig. 19. It can be shown from this figure that the transmitted force is reduced by 2.4 dB by using the impact damper with mass ratio of 0.35.

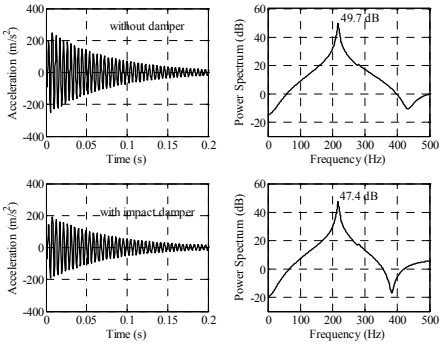

Fig. 18 Simulated acceleration response at point U ($\omega_s = \omega_d$).

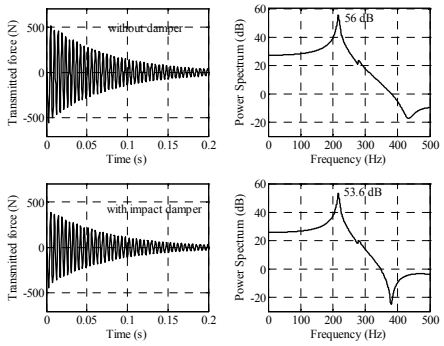

Fig. 19 Simulated force transmission at point U ($\omega_s = \omega_d$).

5. Experimental Validation

In order to validate the simulation results, experiments were carried out using an experimental apparatus. The shape, size, and parameter values are shown in Fig. 1 and Table 1. A photo of the experimental apparatus is shown in Fig. 20. Accelerometer and force transducer sensors were used in the experiment. The accelerometer is used to measure the acceleration response of bed. The acceleration measurement point is located at point B as depicted in Fig. 1. The force sensor is located at one of the floating base springs to measure the force transmitted to the ground.

In this experiment, we cannot measure the forging machine energy directly. However, we can measure the acceleration response and transmitted force of the forging machine. Even though these two parameters are not implicitly indicate the value of forging machine energy, but it can be used to show the portion of forging machine energy being transferred to the momentum exchange impact damper because the square of forging machine acceleration and transmitted force relates proportionally to the kinetic energy and potential energy of the forging machine. As explained in the simulation, the transferred energy is dominated by two modes of vibration, the first elastic mode and the rigid body modes. In this experiment, the reduction of peak levels of these two modes is utilized for the energy analysis.

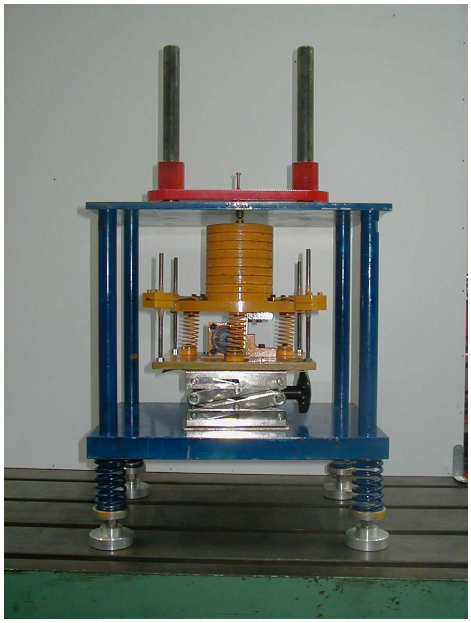

Fig. 20 Photo of experimental apparatus.

The experimental results of the acceleration and transmitted force for the case with the soft support spring and mass ratio of 0.35 are shown in Fig. 21 and 22. These figures show that the acceleration and transmitted force response can be reduced by 3.2 dB and 3.3 dB by using the impact damper. These experimental results and the simulation results in Fig. 10 and 11 are in good agreement, suggesting that the simulation results are reliable.

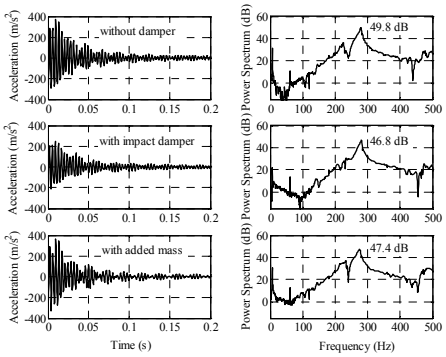

Fig. 21 Experimentally measured acceleration response.

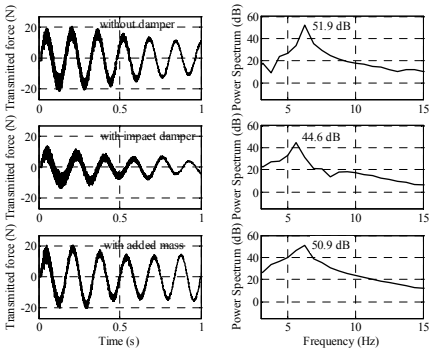

Fig. 22 Experimentally measured force transmission.

6. Conclusion

The vibration power reduction of the forging machine obtained by using the momentum exchange impact damper and the added mass method are about 3 dB and 2 dB, respectively. These values indicate that the vibration of the forging machine reduces by 41.2% and 25.9 % by using the impact damper and the added mass method, respectively. Therefore, it can be concluded that the proposed forging machine impact control method exhibited a high level of vibration isolation and suppression. As shown in the simulation and experimental results, the vibration suppression depends on the mass ratio between the impact damper and the bed, the contact properties and natural frequencies of the forging machine. The energy of the forging machine decreases when the mass ratio increases. In addition, the transfer of energy from the slider to the damper also increases when the excitation frequency ω_s is much larger than the natural frequency of the forging machine. In

the region where the excitation frequency ω_s is lower than the natural frequencies of the bed, the energy stored in the forging machine is not greatly influenced by the mass ratio because the reflected energy of the slider is dominant. However, in the region where the excitation frequency ω_s is higher than the natural frequencies of the bed, the transferred energy from slider to impact damper is dominant and the mass ratio plays a significant role in determining the energy of the forging machine. When one of the natural frequencies of the forging bed is the same as the excitation frequency, the forging machine resonates and the performance of the impact damper is poor.

References

(1) Tanaka, N., and Kikushima, Y., A Study on the dynamic damper with a preview action(1 st report, a principle of the dynamic damper with a preview action), J. Jpn. Soc. Mech. Eng.,(in Japanese), Vol. 52 No.484, C(1986), pp.3176-3183.
(2) Tanaka, N., and Kikushima, Y., A Study on the dynamic damper with a preview action(2 nd report, experiment of the dynamic damper with a preview action), J. Jpn. Soc. Mech. Eng.,(in Japanese), Vol. 53 No.487, C(1987), pp.650-655.
(3) Ceanga, V., and Hurmuzlu, Y., A New look at an old problem: Newtons Cradle, ASME Journal of Applied Mechanics, Vol. 68(2001), pp. 575-583.
(4) Brach, R.M., Mechanical Impact Dynamic : Rigid Body Collision, John Wiley and Sons, New York,1991
(5) Przemieniecky, J.S., Theory of Matrix Structural Analysis. McGraw-Hill, 1967
(6) Bur, M., Dynamische Analyse Linearer und Nichtlinearer Structuren Anhand Theoretischer und Versuchstechnischer Untersuchungen, Diss RWTH Aachen, 1994.
(7) Rajalingham, C., Rakheja, S., Analysis of impact force variation during collision of two bodies using a single degree of freedom system model, J. Sound and Vibration, Vol. 229(2000), pp.823-835